ISSN: (Print) (Online) Journal homepage: <https://www.tandfonline.com/loi/gcoo20>

Oxovanadium and dioxomolybdenum complexes: synthesis, crystal structure, spectroscopic characterization and applications as homogeneous catalysts in sulfoxidation

Hadi Kargar, Azar Kaka-Naeini, Mehdi Fallah-Mehrjardi, Reza Behjatmanesh-Ardakani, Hadi Amiri Rudbari & Khurram Shahzad Munawar

To cite this article: Hadi Kargar, Azar Kaka-Naeini, Mehdi Fallah-Mehrjardi, Reza Behjatmanesh-Ardakani, Hadi Amiri Rudbari & Khurram Shahzad Munawar (2021) Oxovanadium and dioxomolybdenum complexes: synthesis, crystal structure, spectroscopic characterization and applications as homogeneous catalysts in sulfoxidation, *Journal of Coordination Chemistry*, 74:9-10, 1563-1583, DOI: [10.1080/00958972.2021.1915488](https://doi.org/10.1080/00958972.2021.1915488)

To link to this article: <https://doi.org/10.1080/00958972.2021.1915488>



Published online: 05 May 2021.



Submit your article to this journal [↗](#)



Article views: 36



View related articles [↗](#)



View Crossmark data [↗](#)



Oxovanadium and dioxomolybdenum complexes: synthesis, crystal structure, spectroscopic characterization and applications as homogeneous catalysts in sulfoxidation

Hadi Kargar^a , Azar Kaka-Naeini^b, Mehdi Fallah-Mehrjardi^b, Reza Behjatmanesh-Ardakani^b, Hadi Amiri Rudbari^c and Khurram Shahzad Munawar^{d,e} 

^aDepartment of Chemical Engineering, Faculty of Engineering, Ardakan University, Ardakan, Iran;

^bDepartment of Chemistry, Payame Noor University, Tehran, Iran; ^cDepartment of Chemistry, University of Isfahan, Isfahan, Iran; ^dDepartment of Chemistry, University of Sargodha, Punjab, Pakistan; ^eDepartment of Chemistry, University of Mianwali, Mianwali, Pakistan

ABSTRACT

New oxovanadium and dioxomolybdenum Schiff base complexes, $[\text{VO}(\text{L})(\text{OCH}_3)]_n$ and $[\text{MoO}_2(\text{L})(\text{CH}_3\text{OH})]$, were synthesized by treating an ONO donor Schiff base (H_2L) derived by condensation of 3-ethoxysalicylaldehyde and nicotinic hydrazide with oxo and dioxo acetylacetonate salts of vanadium and molybdenum ($\text{VO}(\text{acac})_2$ and $\text{MoO}_2(\text{acac})_2$), respectively. The synthesized ligand and complexes were characterized by FTIR, multinuclear (^1H , ^{13}C) NMR, elemental and single crystal X-ray diffraction analysis. In both complexes, the geometry around the central metal ions was distorted octahedral as revealed by diffraction studies. Theoretical calculations of the synthesized compounds were carried out by DFT at B3LYP/Def2-TZVP level of theory, which showed good correlation with the experimental results. Moreover, the catalytic efficiency of both complexes was investigated by oxidizing aryl and alkyl sulfides in the presence of 30% H_2O_2 in ethanol.

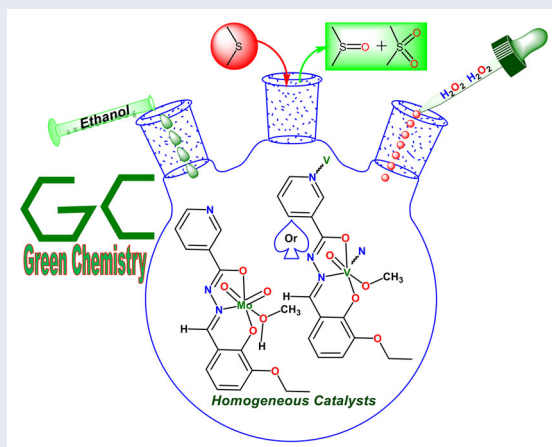
ARTICLE HISTORY

Received 9 December 2020

Accepted 19 March 2021

KEYWORDS

Oxovanadium(V);
dioxomolybdenum(VI);
tridentate Schiff base;
homogeneous catalysis;
sulfoxidation



1. Introduction

Aroylhydrazone-based Schiff base ligands drew much attention during the last few years [1]. These are a new category of tridentate (ONO) ligands which can coordinate with various transition metals. Schiff bases derived from aroylhydrazones and their metal complexes have remarkable applications in biological and industrial fields [2, 3]. These compounds behave as potential pharmacophores for a new series of drugs to be used in many biological processes like inhibition of enzymes, antibacterial, antifungal, antitumor, antileishmanial and antiparasitic activities [4–7]. Among various metal complexes, the oxovanadium(V) and dioxomolybdenum(VI) complexes with such tridentate ligands have prominent positions in the development and progress of chemistry of coordination compounds [8, 9].

The chemistry of vanadium is very rich as it exists in mononuclear (VO^{3+} , VO^{2+}) and dinuclear ($\text{V}_2\text{O}_3^{4+}$) forms. Vanadium and its Schiff base complexes have applications in biochemical processes like insulin-mimetic, antimicrobial, antifungal, haloperoxidation, phosphorylation and alkaline phosphatase inhibition [10–17]. Many of the mononuclear oxovanadium(V) complexes with tridentate ligands having NNO, NNS and NOO donor sites show excellent catalytic roles such as C-H activation, epoxidation, oxidation of alcohols, oxidative halogenation and sulfoxidation by using O_2 and H_2O_2 [18–23].

Molybdenum is an essential element, present in more than 40 different naturally occurring enzymes involved in redox reactions. It is important for the fixation and assimilation of atmospheric nitrogen with the help of bacterial nitrogenase and nitrate reductase [24]. Moreover, molybdoenzymes, sulfite oxidase and aldehyde oxidase are used for oxidation of sulfite and aldehyde, respectively [25]. In addition to the importance of molybdenum complexes in biological process, they have potential to be used as effective catalyst in epoxidation of olefins (styrene and cyclohexane), olefin metathesis, isomerization of allylic alcohol, oxidation of sulfides to sulfoxides and oxidation of amines [26–28]. Coordination of molybdenum with the aroylhydrazones usually generates MoO_2L or MoOL complexes which bear one or two open sites that can be used to enhance the coordination number by binding with substrate molecules. Due to the presence of these vacant sites molybdenum complexes can be regarded as template for numerous enzymatic and catalytic sites [29, 30].

Based on previous research [31–34], we are hereby reporting a new ONO-tridentate ligand (H_2L) prepared by condensing 3-ethoxysalicylaldehyde and nicotinic hydrazide and oxovanadium $[\text{VO}(\text{L})(\text{OCH}_3)]_n$ and dioxomolybdenum $[\text{MoO}_2(\text{L})(\text{CH}_3\text{OH})]$ complexes.

2. Experimental

2.1. Materials and methods

All the chemicals employed in the current work were 99.9% pure and purchased from Sigma-Aldrich and Merck. Elemental analyses were carried out by a Heraeus CHN-O-FLASH EA 1112 instrument. ^1H and ^{13}C NMR spectra were measured at ambient temperature using a BRUKER AVANCE 400 MHz spectrometer employing tetramethylsilane (TMS) as a reference. Coupling constant (J) and chemical shift (δ) values were reported in Hz and

ppm, respectively. Fourier transform infrared spectra of the synthesized compounds were taken with a FTIR spectrometer IRPrestige21 (Shimadzu) as KBr pellets.

2.2. Synthesis

2.2.1. Synthesis of ONO-tridentate Schiff base ligand (H_2L)

Nicotinic hydrazide (1.37 g, 10 mmol) and 3-ethoxysalicylaldehyde (1.66 g, 10 mmol) were dissolved separately in approximately 25 mL of hot methanol. After complete dissolution both solutions were mixed dropwise with continuous stirring. The resulting mixture was refluxed for 3 h and completion of reaction was ensured by monitoring with TLC. On allowing the reaction mixture to attain room temperature, the product precipitated leaving impurities in the solvent. Finally, the desired product was collected by filtration and washed thrice with cold methanol to remove impurities.

H_2L : Yield 76%. Anal. Calc. for $C_{15}H_{15}N_3O_3$: C, 63.15; H, 5.30; N, 14.73, Found: C, 63.04; H, 5.21; N, 14.85%. FTIR (KBr, cm^{-1}): 3570 (ν_{N-H}); 1660 ($\nu_{C=O}$); 1606 ($\nu_{C=N}$); 1477, 1591 ($\nu_{C=C}$); 1161 (ν_{C-O}); 1024 (ν_{N-N}). 1H NMR (400 MHz DMSO- d_6 , ppm): 1.36 [3 H, (H-C15), t, $^3J=6.9$ Hz], 4.07 [4 H, (H-C14), q, $^3J=6.9$ Hz], 6.85 [1 H, (H-C4), t, $^3J=7.9$ Hz], 7.03 [1 H, (H-C3), d, $^3J=7.9$ Hz], 7.18 [1 H, (H-C5), d, $^3J=7.9$ Hz], 7.59 [1 H, (H-C12), dd, $^3J=7.8$ Hz, $^4J=4.8$ Hz], 8.29 [1 H, (H-C13), d, $^3J=7.8$ Hz], 8.67 [1 H, s, (-CH=N)], 8.78 [1 H, (H-C11), dd, $^3J=4.8$ Hz, $^4J=1.4$ Hz], 9.10 [1 H, (H-C10), d, $^4J=1.4$ Hz], 10.79 [1 H, s, (-NH)], 12.24 [1 H, s, (-OH)]. ^{13}C NMR (100 MHz, DMSO- d_6 , ppm): 14.69 (C15), 64.09 (C14) 115.23 (C4), 118.94 (C3), 119.09 (C6), 119.14 (C5), 120.73 (C12), 123.62 (C9), 128.67 (C13), 135.43 (C7), 147.05 (C11), 147.42 (C10), 148.58 (C2), 152.41 (C1), 161.37 (C8).

2.2.2. Synthesis of $[V^VO(L)(OCH_3)]_n$ complex

$[VO(L)(OCH_3)]_n$, where $L = (E)-N'-(3\text{-ethoxy-2-hydroxybenzylidene})\text{nicotino}hydrazide$ (H_2L), was synthesized by treating $[V^VO(acac)_2]$ (1 mmol, 0.265 g, acac = acetylacetonate) with H_2L (1 mmol, 0.285 g) in methanol (50 mL). The mixture was refluxed for 3 h to obtain the precipitate which was filtered off, and then, washed thoroughly with water, methanol and diethyl ether. The precipitate was dried in *vacuo*, and then, crystallized from CH_3OH to obtain green crystals.

$[VO(L)(OCH_3)]_n$: Yield 66%. Anal. Calc. for $C_{16}H_{16}N_3O_5V$: C, 50.41; H, 4.23; N, 11.02, Found: C, 50.34; H, 4.17; N, 11.11%. FTIR (KBr, cm^{-1}): 1604 ($\nu_{C=N}$); 1352 ($\nu_{C=N-N=C}$); 1475, 1552 ($\nu_{C=C}$); 1249 (ν_{C-O}); 1039 (ν_{N-N}); 993 ($\nu_{V=O}$); 588 (ν_{V-O}); 472 (ν_{V-N}).

2.2.3. Synthesis of $[Mo^VO_2(L)(CH_3OH)]$ complex

Equimolar amounts of H_2L (1 mmol, 0.285 g) and $MoO_2(acac)_2$ (1 mmol, 0.330 g) were suspended in 100 mL of methanol in a round bottom flask containing a magnetic bar for stirring to attain uniformity. The suspension was refluxed for 3 h and then 2/3rd of the solvent was evaporated and the remaining solution was cooled over an ice bath giving orange crystals. The crystals were collected by filtration, and then, washed thoroughly with water, methanol and diethyl ether and dried in *vacuo*.

$[MoO_2(L)(CH_3OH)]$: Yield 72%. Anal. Calc. for $C_{16}H_{17}MoN_3O_6$: C, 43.35; H, 3.87; N, 9.48, Found: C, 43.21; H, 3.78; N, 9.56%. FTIR (KBr, cm^{-1}): 3034 (ν_{O-H}) (coordinated

Table 1. Crystal data and refinement parameters for V and Mo complexes.

| Empirical formula | C ₁₆ H ₁₆ N ₃ O ₅ V | C ₁₆ H ₁₇ MoN ₃ O ₆ |
|--|---|---|
| Formula weight | 381.26 | 443.26 |
| Temperature/K | 298(2) | 298(2) |
| Crystal system | Monoclinic | Monoclinic |
| Space group | P2 ₁ /c | P2 ₁ /c |
| a/Å | 11.963(2) | 8.2916(17) |
| b/Å | 10.797(2) | 16.046(3) |
| c/Å | 26.294(5) | 13.541(3) |
| α/° | 90 | 90 |
| β/° | 99.35(3) | 95.16(3) |
| γ/° | 90 | 90 |
| Volume/Å ³ | 3351.2(12) | 1794.3(6) |
| Z | 8 | 4 |
| ρ _{calc} (mg/mm ³) | 1.511 | 1.641 |
| μ (mm ⁻¹) | 0.624 | 0.769 |
| F(000) | 1568 | 896 |
| θ range for data collection (°) | 2.556 to 24.998 | 2.466 to 24.991 |
| Index ranges | -14 ≤ h ≤ 14, -12 ≤ k ≤ 12, -31 ≤ l ≤ 31 | -9 ≤ h ≤ 9, -19 ≤ k ≤ 0, -16 ≤ l ≤ 16 |
| Reflections collected | 19440 | 5698 |
| Independent reflections, R(int) | 5884 (0.0957) | 3150 (0.0265) |
| Data / restraints / parameters | 5884 / 1 / 453 | 3150 / 1 / 240 |
| Goodness-of-fit on F ² | 0.705 | 0.746 |
| Final R indexes [I > 2σ (I)] | R ₁ = 0.0431, wR ₂ = 0.0807 | R ₁ = 0.0281, wR ₂ = 0.0541 |
| Final R indexes [all data] | R ₁ = 0.1187, wR ₂ = 0.0916 | R ₁ = 0.0520, wR ₂ = 0.0565 |
| Largest peak and deepest hole (e.Å ⁻³) | -0.369, 0.431 | -0.395, 0.606 |

methanol); 1610 (v_{C=N}); 1448 (v_{C=N-N=C}); 1448, 1527 (v_{C=C}); 1257 (v_{C-O}); 1029 (v_{N-N}); 937 (v_{O=Mo=O}) *asym*; 918 (v_{O=Mo=O}) *sym*; 597 (v_{Mo-O}); 472 (v_{Mo-N}). ¹H NMR (400 MHz, DMSO-d₆, ppm): 1.35 [3 H, (H-C15), t, ³J = 6.9 Hz], 4.08 [4 H, (H-C14), q, ³J = 6.9 Hz], 7.02 [1 H, (H-C4), t, ³J = 7.9 Hz], 7.26 [1 H, (H-C3), d, ³J = 7.9 Hz], 7.33 [1 H, (H-C5), d, ³J = 7.9 Hz], 7.56 [1 H, (H-C12), dd, ³J = 7.9 Hz, ³J = 4.8 Hz], 8.31 [1 H, (H-C13), dt, ³J = 7.9 Hz, ⁴J = 1.7 Hz], 8.76 [1 H, (H-C11), d, ³J = 4.8 Hz], 8.98 [1 H, s, (CH = N)], 9.15 [s, 1 H, (H-C10)]. ¹³C NMR (100 MHz, DMSO-d₆, ppm): 14.69 (C15), 64.35 (C14), 118.87 (C4), 120.56 (C3), 121.62 (C6), 123.94 (C5), 125.66 (C12), 126.09 (C9), 135.37 (C13), 147.59 (C1), 148.72 (C2), 149.48 (C10), 152.36 (C11), 156.80 (C7), 167.14 (C8).

2.3. X-Ray crystallographic data collection and structure determination of the complexes

Single crystal X-ray studies of oxovanadium and dioxomolybdenum complexes were carried out on a STOE IPDS-II diffractometer using Mo-Kα radiations monochromated by graphite. The data were collected at 298(2) K in a series of ω scans in 1° oscillations and integrated using the Stöe X-Area [35] software package. A numerical absorption correction was applied using X-RED [36] and X-SHAPE [37] software for the Mo complex. For the V complex, absorption corrections based on multiscan were applied [38]. The data were corrected for Lorentz and polarization effects. The structures were solved by direct methods using SIR2004 [39]. Non-hydrogen atoms were refined anisotropically by full-matrix least-squares on F² using SHELXL [40]. The crystallographic data of the complexes are provided in Table 1 while selected bond lengths and angles are listed in Table 2.

Table 2. The selected experimental bond lengths (Å) and angles (°) in V and Mo complexes.

| | | | |
|-------------------|------------|-----------------|------------|
| V complex | | | |
| V(1)–O(1) | 1.862(3) | O(4)–V(1)–O(3) | 102.86(16) |
| V(1)–O(2) | 1.974(3) | O(4)–V(1)–O(1) | 100.15(14) |
| V(1)–O(3) | 1.763(3) | O(3)–V(1)–O(1) | 104.99(13) |
| V(1)–O(4) | 1.578(3) | O(4)–V(1)–O(2) | 97.70(13) |
| V(1)–N(1) | 2.112(4) | O(3)–V(1)–O(2) | 91.18(13) |
| V(1)–N(3) | 2.458(3) | O(1)–V(1)–O(2) | 152.45(12) |
| N(1)–C(7) | 1.294(5) | O(4)–V(1)–N(1) | 95.12(15) |
| N(1)–N(5) | 1.415(4) | O(3)–V(1)–N(1) | 158.10(14) |
| C(1)–O(1) | 1.337(5) | O(1)–V(1)–N(1) | 83.70(13) |
| C(8)–O(2) | 1.304(5) | O(2)–V(1)–N(1) | 73.92(13) |
| V(2)–O(6) | 1.853(3) | O(6)–V(2)–N(4) | 80.26(13) |
| V(2)–O(7) | 1.947(3) | O(7)–V(2)–N(4) | 73.80(12) |
| V(2)–O(8) | 1.594(3) | O(8)–V(2)–N(4) | 91.99(15) |
| V(2)–O(9) | 1.765(3) | O(9)–V(2)–N(4) | 163.60(15) |
| V(2)–N(4) | 2.448(4) | N(4)–V(2)–N(7) | 82.54(13) |
| V(2)–N(7) | 2.134(3) | O(8)–V(2)–N(7) | 174.39(14) |
| Mo complex | | | |
| Mo(1)–O(1) | 2.012(2) | O(1)–Mo(1)–O(2) | 148.73(10) |
| Mo(1)–O(2) | 1.9290(19) | O(1)–Mo(1)–O(3) | 95.09(11) |
| Mo(1)–O(3) | 1.695(2) | O(1)–Mo(1)–O(4) | 98.91(11) |
| Mo(1)–O(4) | 1.695(3) | O(1)–Mo(1)–O(6) | 80.10(9) |
| Mo(1)–O(6) | 2.309(3) | O(3)–Mo(1)–O(6) | 85.31(12) |
| Mo(1)–N(2) | 2.235(3) | O(4)–Mo(1)–O(6) | 168.30(11) |
| N(2)–C(7) | 1.297(4) | O(1)–Mo(1)–N(2) | 71.69(9) |
| N(1)–N(2) | 1.409(4) | O(2)–Mo(1)–N(2) | 101.74(13) |
| C(9)–O(1) | 1.313(4) | O(3)–Mo(1)–N(2) | 160.95(15) |
| C(1)–O(2) | 1.360(4) | O(4)–Mo(1)–N(2) | 92.16(12) |

2.4. General procedure for the oxidation of sulfides catalyzed by the V and Mo complexes

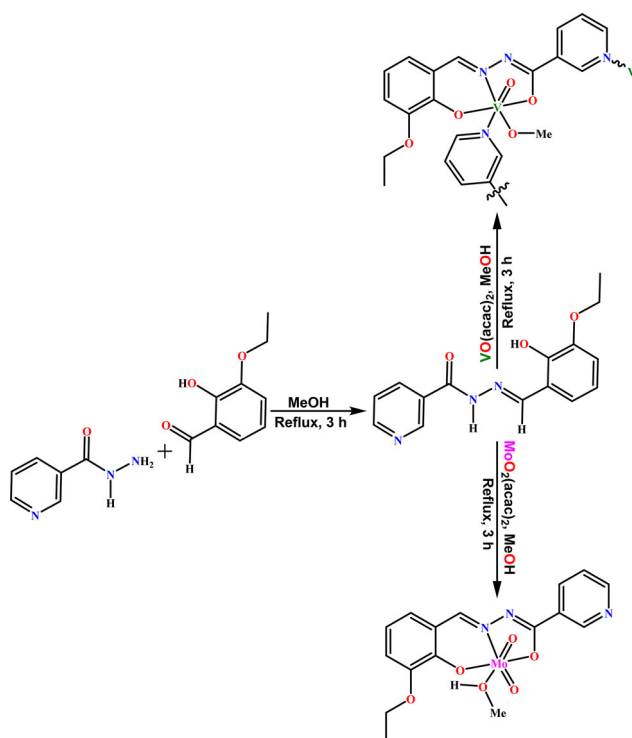
To a solution of sulfide (1 mmol) and 30% aqueous H₂O₂ (2 mmol) in EtOH (10 mL), [VO(L)(OCH₃)_n] (0.004 mmol) or [MoO₂(L)(CH₃OH)] (0.006 mmol) was added and the reaction mixture was refluxed with continuous stirring for intervals of times. The catalytic reaction was scrutinized by TLC (eluent, *n*-hexane:ethyl acetate, 5:2) and the yield of products was determined by GC analysis. The products were purified by chromatography over silica gel with a 70:30 mixture of *n*-hexane and ethyl acetate as eluent. All products were known compounds and identified by comparing their FTIR and NMR spectra with those of authentic samples.

3. Results and discussion

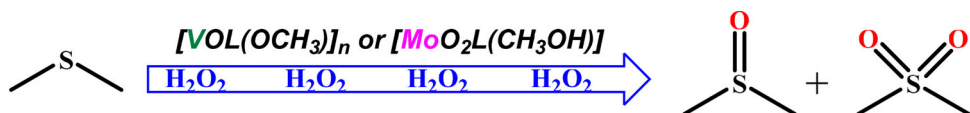
A tridentate Schiff base (H₂L) was prepared by treating nicotinic hydrazide with 3-ethoxysalicylaldehyde in methanol. Reaction of VO(acac)₂ and MoO₂(acac)₂ with H₂L in methanol under reflux produces the targeted metal complexes (Scheme 1). After synthesis and characterization, the catalytic effectiveness of the complexes were checked by oxidizing various sulfides using 30% H₂O₂ (Scheme 2).

3.1. ¹H NMR and ¹³C NMR spectra

The ¹H and ¹³C NMR data of H₂L and its Mo complex in DMSO are presented in the Experimental section and spectra are shown in Figures 1–3. Two signals at δ = 12.24



Scheme 1. Syntheses of H_2L , $[VO(L)(OCH_3)]_n$ and $[MoO_2(L)(CH_3OH)]$.



Scheme 2. Catalytic oxidation of alkyl sulfides in the presence of H_2O_2 by $[VO(L)(OCH_3)]_n$ and $[MoO_2(L)(CH_3OH)]$.

and 10.79 ppm in the 1H NMR spectrum of H_2L which correspond to OH (phenolic) and NH protons, respectively, disappear on treatment with Mo salt, demonstrating that the sites of coordination are phenolato and enolato oxygens of the ligand. This also ascertains the occurrence of *keto-imine* tautomerism upon complexation. Moreover, a singlet of azomethine proton ($-HC=N$) at $\delta = 8.67$ ppm observed in the spectra of H_2L shifted downfield at $\delta = 8.98$ ppm showing deshielding due to the decrease in the electronic density upon the coordination of azomethine nitrogen. This is in accord with the FTIR spectrum of the complex, where $\nu(HC=N)$ appears at higher wavenumber in comparison with the corresponding ligand. There is a slight shift in the positions of aromatic protons in the NMR spectra of the ligand upon complex formation. The ethoxy part of the ligand gives a quartet at $\delta = 4.07$ ppm [$^3J(H,H) = 6.9$ Hz] due to $-OCH_2$ protons and a triplet at $\delta = 1.36$ ppm [$^3J(H,H) = 6.9$ Hz] because of the $-CH_3$ protons coupling with each other. The aliphatic protons failed to exhibit any noticeable shifts in their positions upon complexation.

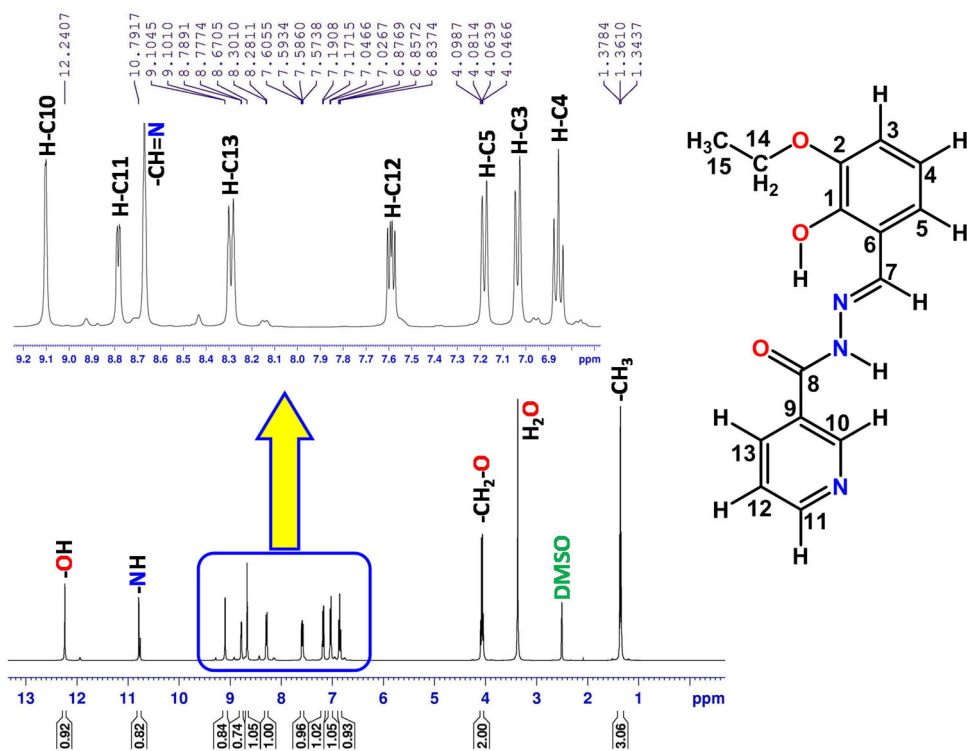


Figure 1. ^1H NMR spectrum of H_2L in DMSO-d_6 .

The ^{13}C NMR spectra of H_2L and its Mo complex are shown in Figure 3. The signals for the carbonyl, phenolic and methine carbon were observed at 161.3, 152.4 and 135.4 ppm, respectively. The chemical shift values of the carbons present close to the coordinating atoms (i.e. C8, C1 and C7) showed appreciable change in their position due to coordination-induced shifts, confirming the association of these functionalities in coordination. The other aromatic carbons of ligand and Mo complex appeared in their respective regions according to the literature. Hence, ^{13}C NMR spectra also support the conclusions made from ^1H NMR spectral data.

3.2. FTIR spectra

FTIR spectra of H_2L and its oxovanadium and dioxomolybdenum complexes are shown in Figure 4. Comparison of the FTIR spectra of the compounds was carried out to confirm the sites of coordination. FTIR spectra of H_2L showed bands at 3570 and 1660 cm^{-1} which correspond to the stretching vibrations of $\nu(\text{NH})$ and $\nu(\text{C}=\text{O})$. These bands disappeared in spectra of the complexes, in accord with enolization of the amide functional group and deprotonation for coordination to metal ions. X-ray diffraction data also confirm the mode of coordination of the ligand. The stretching vibration of azomethine ($-\text{HC}=\text{N}$) in H_2L appears at 1606 cm^{-1} and slightly shifts on complexation. New bands at 1257 and 1249 cm^{-1} are attributed to enolic $\nu(\text{C}-\text{O})$ moiety in molybdenum and vanadium complexes, respectively. The appearance of two new bands at 937 and 918 cm^{-1} are assigned to symmetric and asymmetric stretching

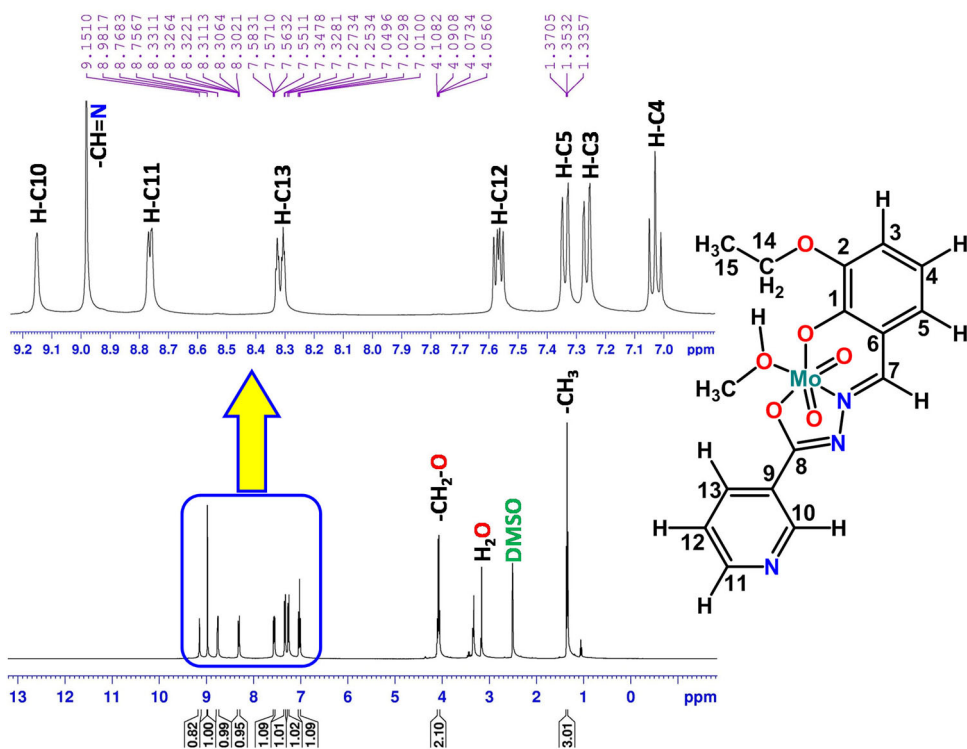


Figure 2. ^1H NMR spectrum of $[\text{MoO}_2(\text{L})(\text{CH}_3\text{OH})]$ in DMSO-d_6 .

vibrations of the *cis*- $\text{Mo}(\text{O})_2$, in accord with similar structures reported [41, 42]. Similarly, oxovanadium complex also gives its characteristic peak of $\text{V}=\text{O}$ at 993 cm^{-1} , close to the values of reported oxovanadium Schiff base complexes [43–45]. Some new M–O and M–N peaks are present at 597 and 472 cm^{-1} for Mo complex and at 588 and 472 cm^{-1} for V complex, respectively, in agreement to reported complexes [43–46].

3.3. Crystal structure determination

The molecular structure along with the atom numbering scheme of the vanadium complex is shown in Figure 5. The complex is a neutral, one-dimensional coordination polymer of oxovanadium(V). The two crystallographically independent molecules of the vanadium complex are linked by the nicotinic moiety from the ligand through a V1–N3 bond to build the repetitive unit. The phenolic oxygen (O1), imino nitrogen (N1) and enolic oxygen (O2) of the nicotinothrazone ligand along with methoxy oxygen (O3) make the basal plane while the axial positions are oxygen (O4) of oxido and nitrogen (N3) of the nicotinothrazone ligand from the second unit of oxovanadium complex. Hence, each V(V) center is six coordinate in a distorted octahedron.

The ligand coordinates tridentate (ONO) as a dianion as apparent from N1–C7 and O2–C9 bond lengths. The abnormal bond values indicate the presence of the enolate form of the amide groups. The V–O, V–N and $\text{V}=\text{O}$ bonds are within normal ranges and similar to those observed in similar oxovanadium(V) complexes [5, 47, 48]. Due to

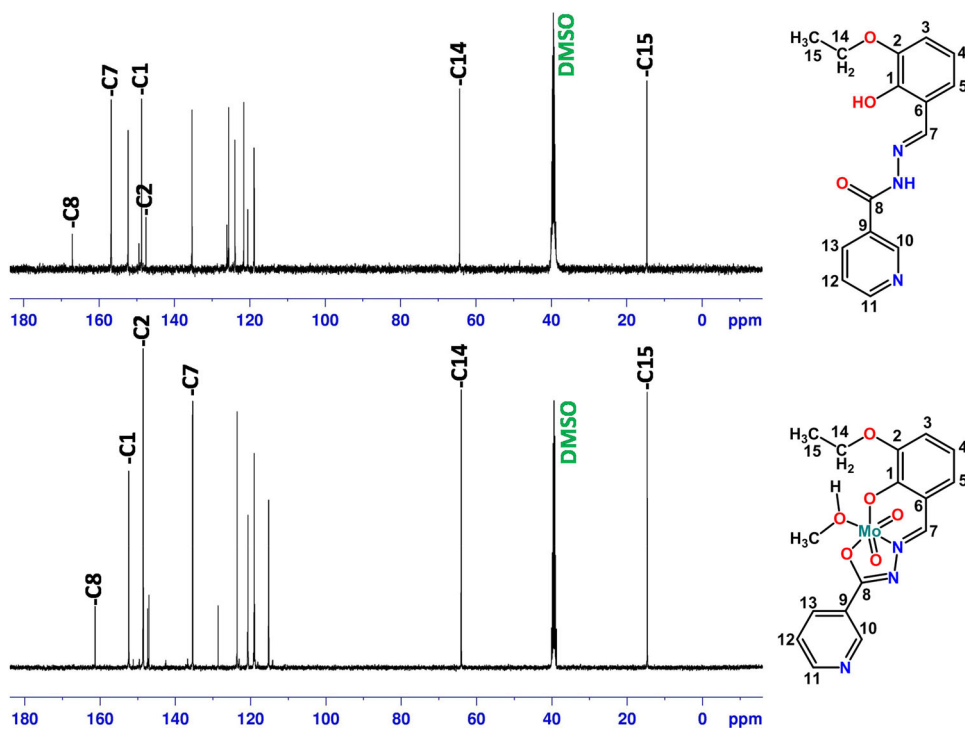


Figure 3. ^{13}C NMR spectra of H_2L and $[\text{MoO}_2(\text{L})(\text{CH}_3\text{OH})]$ in DMSO-d_6 .

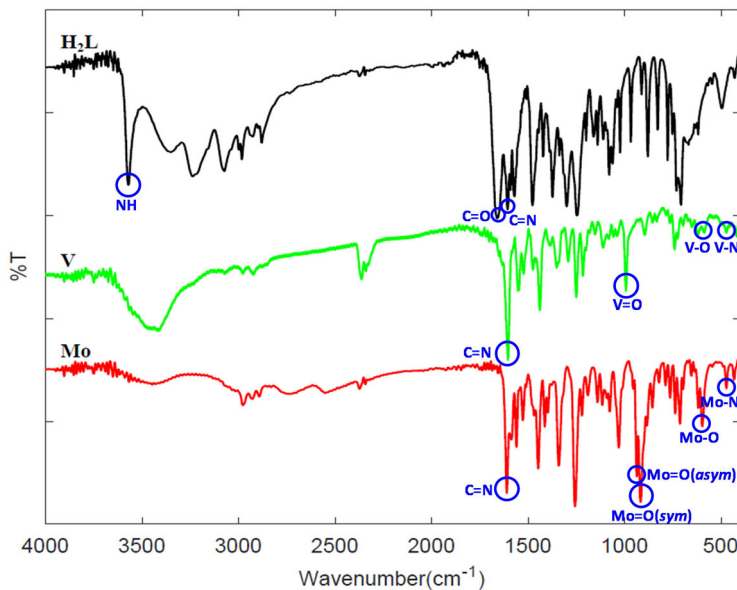


Figure 4. FTIR spectra of H_2L and its V and Mo complexes.

the *trans* effect of the oxo group, the distance between V2 and N3 of the nicotinyl moiety (2.458(3) Å) is longer than the usual bond length, indicating weak association between two units to form a polymeric structure. In contrast to this, the V1-O4 bond distance

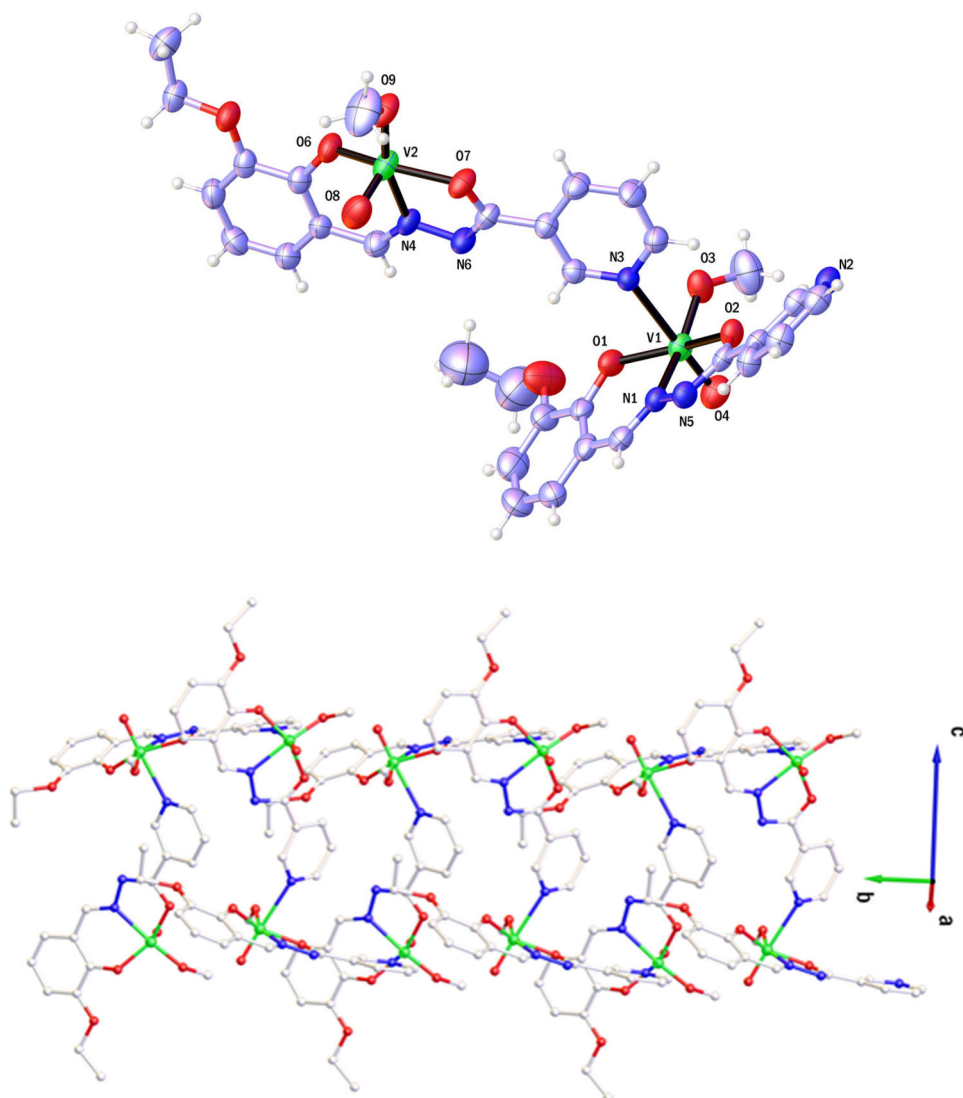


Figure 5. ORTEP view of the asymmetric unit of $[\text{VO}(\text{L})(\text{OCH}_3)]_n$ (upper) and one-dimensional polymeric chain (lower) shown in ball and stick mode. Thermal ellipsoids are drawn at the 50% probability level, while the hydrogen size is arbitrary.

(1.578(3) Å) is shorter, which indicates a double bond. These polymeric complexes in which two complex units coordinate through nicotinic nitrogen are few in number.

The molecular structure of the dioxomolybdenum complex is shown in Figure 6. The coordination geometry around the molybdenum center can be described as distorted octahedral in which two *cis* positions are occupied by the two oxo groups and a tridentate dianionic hydrazone Schiff base. The sixth coordination site of molybdenum is occupied by the oxygen from the methanol forming the mononuclear complex. The distance between molybdenum and the oxygen of methanol, Mo1-O6 of 2.309(3) Å, represents the largest bond length within the distorted octahedron. The elongated Mo1–O6 bond length *trans* to oxo O1 indicates weak coordination of

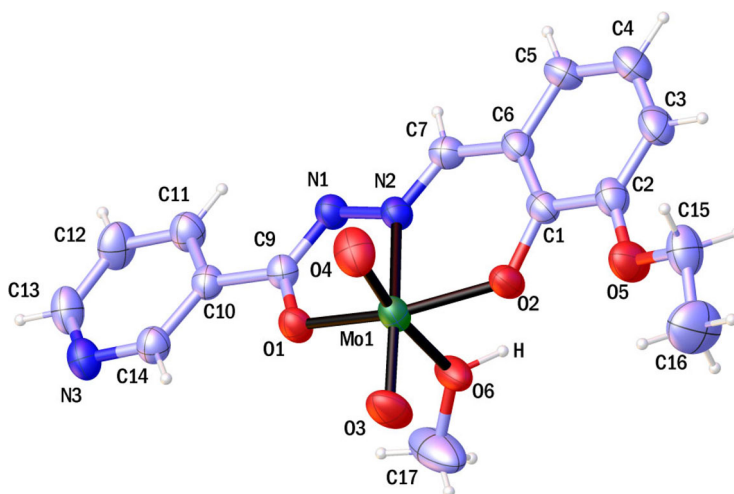


Figure 6. ORTEP view of the asymmetric unit of $[\text{MoO}_2(\text{L})(\text{CH}_3\text{OH})]$. Thermal ellipsoids are drawn at the 50% probability level, while the hydrogen size is arbitrary.

methanol at the axial position due to the strong π -donor character of the *trans* oxo, as commonly observed [49]. The distortion of the octahedral coordination can also be substantiated from the bond angles related to the Mo ions which are summarized in Table 2. The Mo–O and Mo–N bond lengths in the complex are comparable to those observed in other oxomolybdenum complexes with hydrazone ligands [49–51]. As with previously reported bond lengths of N1–N2 [1.409(4) Å] and iminic N1–C7 [1.297(4) Å] groups increased upon coordination to molybdenum. The two Mo=O bond distances and the subtended O(1)=Mo(1)=O(2) are comparable to those previously reported for molybdenum complexes [49–51].

3.4. Theoretical results

3.4.1. Optimized structural parameters

Geometry optimizations of the ligand and its complexes are performed by DFT at the B3LYP/Def2-TZVP level of theory in the gas phase. The optimized structures of the compounds are shown in Figure 7 and the selected calculated bond lengths and angles of the V and Mo complexes are listed in Table 3. On comparing the data in Tables 2 and 3, theoretical data are analogous to the experimental results. The differences between the theoretical and experimental values are due to the fact that the experimental data belong to the molecules in the solid state, while the calculated values correspond to the molecules in the gaseous phase.

By comparing the Gibbs free energy (G) of both *enol* and *keto* forms of H_2L in the gas and solution phases, the *keto* form is more stable than the *enol* form in both phases (Table 4).

3.4.2. Electronic properties

The frontier molecular orbital energy levels and their energy gaps ($\Delta E = E_{\text{LUMO}} - E_{\text{HOMO}}$) are often used to describe the stability and the chemical reactivity of the

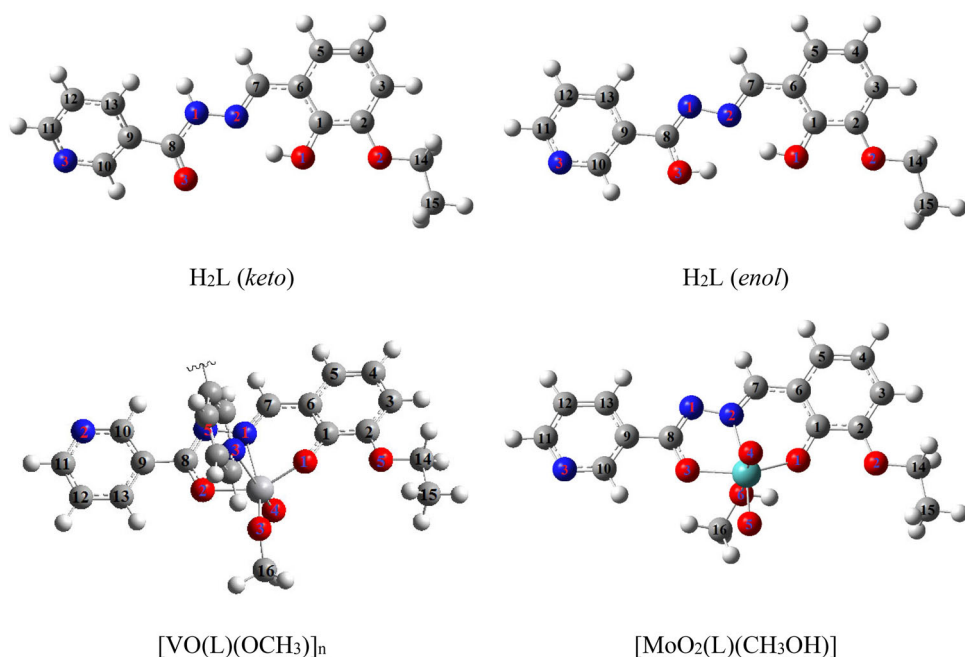


Figure 7. Optimized structures of H_2L (*keto* and *enol* forms), $[\text{VO}(\text{L})(\text{OCH}_3)]_n$ and $[\text{MoO}_2(\text{L})(\text{CH}_3\text{OH})]$.

Table 3. The selected calculated bond lengths (Å) and angles (°) in V and Mo complexes.^a

| | | | |
|-------------------|-------|-----------------|--------|
| V complex | | | |
| V(1)–O(1) | 1.857 | O(4)–V(1)–O(3) | 103.19 |
| V(1)–O(2) | 1.959 | O(4)–V(1)–O(1) | 101.55 |
| V(1)–O(3) | 1.777 | O(3)–V(1)–O(1) | 103.17 |
| V(1)–O(4) | 1.573 | O(4)–V(1)–O(2) | 100.21 |
| V(1)–N(1) | 2.160 | O(3)–V(1)–O(2) | 93.86 |
| V(1)–N(3) | 2.635 | O(1)–V(1)–O(2) | 148.35 |
| N(1)–C(7) | 1.290 | O(4)–V(1)–N(1) | 95.01 |
| N(1)–N(5) | 1.372 | O(3)–V(1)–N(1) | 159.46 |
| C(1)–O(1) | 1.320 | O(1)–V(1)–N(1) | 82.08 |
| C(8)–O(2) | 1.301 | O(2)–V(1)–N(1) | 73.36 |
| V(2)–O(6) | 1.850 | O(6)–V(2)–N(4) | 82.30 |
| V(2)–O(7) | 1.953 | O(7)–V(2)–N(4) | 73.48 |
| V(2)–O(8) | 1.571 | O(8)–V(2)–N(4) | 96.10 |
| V(2)–O(9) | 1.780 | O(9)–V(2)–N(4) | 158.25 |
| V(2)–N(4) | 2.152 | N(4)–V(2)–N(7) | 81.03 |
| V(2)–N(7) | 2.752 | O(8)–V(2)–N(7) | 176.65 |
| Mo complex | | | |
| Mo(1)–O(1) | 2.007 | O(1)–Mo(1)–O(2) | 143.06 |
| Mo(1)–O(2) | 1.950 | O(1)–Mo(1)–O(3) | 97.04 |
| Mo(1)–O(3) | 1.700 | O(1)–Mo(1)–O(4) | 101.60 |
| Mo(1)–O(4) | 1.688 | O(1)–Mo(1)–O(6) | 78.33 |
| Mo(1)–O(6) | 2.579 | O(3)–Mo(1)–O(6) | 80.57 |
| Mo(1)–N(2) | 2.288 | O(4)–Mo(1)–O(6) | 171.66 |
| N(2)–C(7) | 1.289 | O(1)–Mo(1)–N(2) | 70.43 |
| N(1)–N(2) | 1.373 | O(2)–Mo(1)–N(2) | 79.21 |
| C(9)–O(1) | 1.317 | O(3)–Mo(1)–N(2) | 155.22 |
| C(1)–O(2) | 1.333 | O(4)–Mo(1)–N(2) | 96.02 |

^aThe number of atoms is based on the numbering of the X-ray structure.

compounds. The HOMO and LUMO plots of V and Mo complexes as well as the free ligand drawn by B3LYP/Def2-TZVP level of theory are shown in Figure 8. The energy

Table 4. Sum of the electronic and the zero-point energy (E^{ZPE}), enthalpy (H) and Gibbs free energy (G) of the ligand.

| | H ₂ L (<i>keto</i>) | | H ₂ L (<i>enol</i>) | |
|------------------|----------------------------------|----------------|----------------------------------|----------------|
| | Gas phase | Solution phase | Gas phase | Solution phase |
| E^{ZPE} | -970.620 | -970.640 | -970.615 | -970.627 |
| H | -970.560 | -970.614 | -970.596 | -970.601 |
| G | -970.669 | -970.703 | -970.664 | -970.690 |

All values are in Hartree units.

¹Hartree = 627.5095 kcal.mol⁻¹.

gaps for the H₂L (*keto*), H₂L (*enol*), [VO(L)(OCH₃)_n] and [MoO₂(L)(CH₃OH)] were 3.896, 3.748, 3.037 and 3.335 eV, respectively. The energy gap of H₂L (*keto*) is slightly greater than that of H₂L (*enol*), which can be attributed to higher stability of *keto* tautomeric form of the ligand.

3.4.3. Molecular electrostatic potential

Molecular electrostatic potential (MEP) is a very useful property for chemical activities of the molecules. The three-dimensional MEP diagrams have been specified by the regions of high electronic density with red (electrophilic reactivity) and electron deficient regions with blue (nucleophilic reactivity). The MEP diagrams and values of electrostatic potentials of H₂L and its complexes are presented in Figure 9. There is a significant difference between the values of electrostatic potential for *enol* and *keto* forms of H₂L. In *keto* form, the oxygens of the phenolic and carbonyl groups, with electrostatic potential value of approximately 57 kcal.mol⁻¹, are the most reactive nucleophilic centers for coordination with metal ions, while in *enol* form, the two hydroxyl groups, specified by blue color, correspond to the electrophilic sites with a positive value of electrostatic potential, i.e. approximately 37 kcal.mol⁻¹. In the oxovanadium and dioxomolybdenum complexes the electrostatic potential values are approximately 35 and approximately 42 kcal.mol⁻¹, respectively. Hence, the metal ion is the center of positive electrostatic potential and represented by blue color which means it is a good candidate for attack by a nucleophile.

3.4.4. Mulliken atomic charge

The calculated Mulliken charges on the active sites of the oxovanadium and dioxomolybdenum complexes as well as on H₂L are presented in Table 5. The Mulliken charge on the metal ions are +1.170 and +1.473 for V and Mo complexes, respectively, which are considerably less than that of formal charges, +5 for V and +6 for Mo. This difference indicates that a significant amount of charge density is transferred from the ligand to the metal atoms. C1, C2 and C8 have the highest positive values of atomic charges as these C-sites are adjacent to the highly electronegative O-atoms. Also, the maximum variation in the charge density is shown at O1, O3, N2, C1 and C8, after the complexation with vanadium and molybdenum.

3.4.5. Theoretical study of FTIR spectra

Some selected calculated and experimental vibrational modes of H₂L and its V and Mo complexes are listed in Table 6 with a good correlation between theoretical and experimental results. This indicates similarity between the structures of the compounds in the gaseous and solid states.

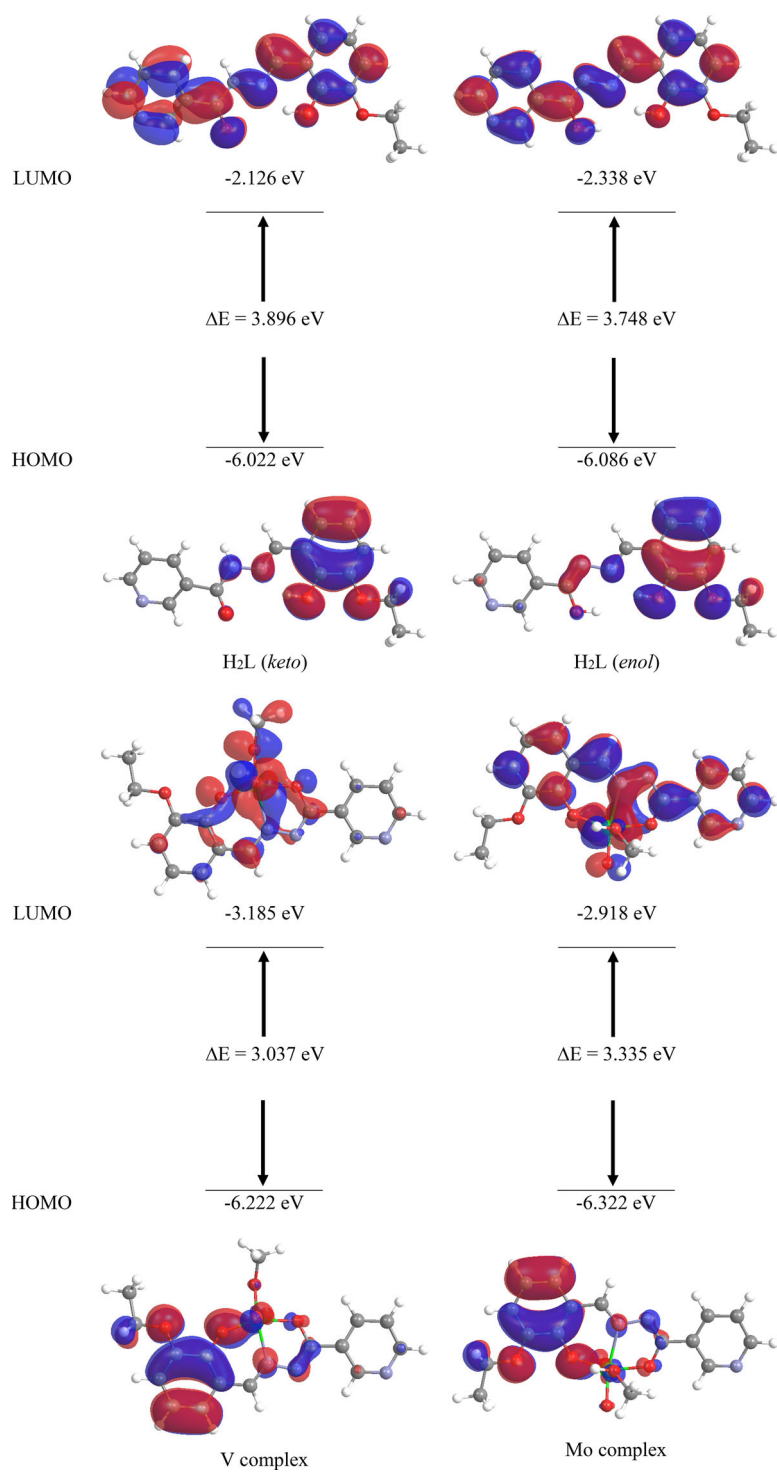


Figure 8. DFT-optimized frontier molecular orbitals of H₂L (*keto* and *enol*), V and Mo complexes.

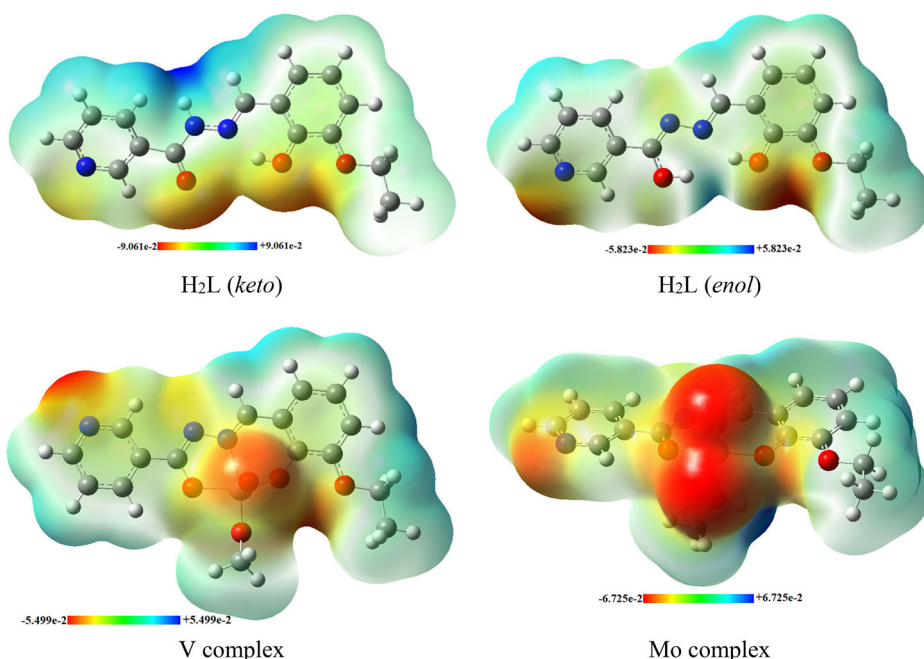


Figure 9. Molecular electrostatic potential (MEP) for H₂L (*keto* and *enol*), V and Mo complexes with color range along with scale.

Table 5. The Mulliken atomic charges of H₂L and its V and Mo complexes.

| Atoms | H ₂ L ligand | V complex | Mo complex | Atoms | H ₂ L ligand | V complex | Mo complex |
|-------|-------------------------|-----------|------------|-------|-------------------------|-----------|------------|
| M1 | – | 1.170 | 1.473 | C4 | –0.156 | –0.129 | –0.126 |
| O1 | –0.369 | –0.525 | –0.572 | C5 | –0.194 | –0.225 | –0.229 |
| O2 | –0.246 | –0.252 | –0.251 | C6 | 0.090 | 0.084 | 0.115 |
| O3 | –0.323 | –0.519 | –0.543 | C7 | –0.008 | –0.040 | –0.017 |
| O4 | – | –0.438 | –0.572 | C8 | 0.276 | 0.430 | 0.419 |
| O5 | – | –0.479 | –0.539 | C9 | 0.065 | 0.019 | 0.029 |
| O6 | – | – | –0.447 | C10 | –0.070 | –0.077 | –0.074 |
| N1 | –0.178 | –0.259 | –0.249 | C11 | –0.024 | –0.024 | –0.024 |
| N2 | –0.160 | –0.020 | –0.063 | C12 | –0.110 | –0.095 | –0.098 |
| N3 | –0.199 | –0.203 | –0.204 | C13 | –0.179 | –0.137 | –0.147 |
| C1 | 0.136 | 0.315 | 0.287 | C14 | –0.040 | –0.042 | –0.046 |
| C2 | 0.204 | 0.230 | 0.239 | C15 | –0.313 | –0.316 | –0.316 |
| C3 | –0.208 | –0.219 | –0.222 | C16 | – | –0.155 | –0.146 |

The N–H stretch frequency in theoretical (3399 cm^{-1}) and experimental data (3570 cm^{-1}) are far apart. The same set of patterns is manifested in the illustration of C=O stretching frequency where theoretical value appeared at 1754 cm^{-1} , which is away from the experimental data at 1660 cm^{-1} . This huge difference of vibrational frequencies in the values may be due to the involvement of these groups (N–H and C=O) in hydrogen bonding in the solid state.

3.4.6. Theoretical study of ¹H and ¹³C NMR spectra

The experimental and calculated ¹H and ¹³C NMR chemical shifts of H₂L and its complexes are given in Table 7. It is evident from the table that the theoretical data agree with the experimental findings.

Table 6. Selected experimental and calculated FTIR vibrational frequencies (cm^{-1}) of H_2L and its V and Mo complexes.

| Assignment | H_2L ligand | | | V complex | | | Mo complex | | |
|------------|-----------------------------|-------|---------------------------------|-----------|-------|---------------------------------|------------|-------|---------------------------------|
| | Exp. | Calc. | Relative error (%) ^a | Exp. | Calc. | Relative error (%) ^a | Exp. | Calc. | Relative error (%) ^a |
| NH | 3570 | 3399 | -4.79 | – | – | – | – | – | – |
| C=O | 1660 | 1754 | 5.66 | – | – | – | – | – | – |
| HC=N | 1606 | 1671 | 4.05 | 1604 | 1653 | 3.05 | 1610 | 1662 | 3.23 |
| C=C | 1591 | 1551 | -2.51 | 1552 | 1593 | 2.64 | 1527 | 1556 | 1.90 |
| | 1477 | 1492 | 1.02 | 1475 | 1472 | -0.20 | 1448 | 1474 | 1.80 |
| C-O | 1246 | 1261 | 1.20 | 1249 | 1311 | 4.96 | 1257 | 1290 | 2.63 |
| M=O | – | – | – | 993 | 1043 | 5.04 | 937 | 986 | 5.23 |
| | | | | | | | 918 | 915 | -0.33 |
| M-O | – | – | – | 588 | 608 | 3.40 | 597 | 602 | 0.84 |
| M-N | – | – | – | 472 | 484 | 2.54 | 472 | 476 | 0.85 |

^aRelative error (%) = $(X^{\text{Calc}} - X^{\text{Exp}}) * 100 / X^{\text{Exp}}$.

Table 7. Experimental and calculated ^1H and ^{13}C -NMR shifts of H_2L and its Mo complex (ppm).

| | H_2L ligand | | Mo complex | |
|---------------------|-----------------------------|------------|--------------|------------|
| | Experimental | Calculated | Experimental | Calculated |
| ^1H NMR | | | | |
| OH | 12.24 | 11.85 | – | – |
| NH | 10.79 | 9.06 | – | – |
| CH(10) | 9.10 | 9.53 | 9.15 | 9.53 |
| CH(11) | 8.78 | 9.14 | 8.76 | 9.10 |
| HC=N | 8.67 | 8.51 | 8.98 | 9.02 |
| CH(13) | 8.29 | 8.28 | 8.31 | 8.94 |
| CH(12) | 7.59 | 7.74 | 7.56 | 7.74 |
| CH(5) | 7.18 | 7.23 | 7.33 | 7.45 |
| CH(3) | 7.03 | 7.22 | 7.26 | 7.41 |
| CH(4) | 6.85 | 7.22 | 7.02 | 7.43 |
| CH(14) | 4.07 | 4.11* | 4.08 | 4.10* |
| CH(15) | 1.36 | 1.52* | 1.35 | 1.52* |
| ^{13}C NMR | | | | |
| CH(8) | 161.37 | 169.19 | 167.14 | 177.27 |
| CH(1) | 152.41 | 158.71 | 147.59 | 159.62 |
| CH(2) | 148.58 | 156.79 | 148.72 | 157.05 |
| CH(10) | 147.42 | 158.87 | 149.48 | 157.95 |
| CH(11) | 147.05 | 161.28 | 152.36 | 161.32 |
| CH(7) | 135.43 | 156.34 | 156.80 | 165.14 |
| CH(13) | 128.67 | 140.35 | 135.37 | 143.62 |
| CH(9) | 123.62 | 136.59 | 126.09 | 133.08 |
| CH(12) | 120.73 | 129.68 | 125.66 | 129.90 |
| CH(5) | 119.14 | 128.74 | 123.94 | 131.62 |
| CH(6) | 119.09 | 124.30 | 121.62 | 127.22 |
| CH(3) | 118.94 | 119.21 | 120.56 | 123.63 |
| CH(4) | 115.23 | 124.42 | 118.87 | 128.94 |
| CH(14) | 64.09 | 69.93 | 64.35 | 70.56 |
| CH(15) | 14.69 | 17.31 | 14.69 | 17.20 |

*Average values obtained from calculations.

3.5. General procedure for oxidation of sulfides catalyzed by $[\text{VO}(\text{L})(\text{OCH}_3)]_n$ and $[\text{MoO}_2(\text{L})(\text{CH}_3\text{OH})]$ under reflux

To a 10 mL of ethanolic solution of diphenyl sulfides (1 mmol), $[\text{VO}(\text{L})(\text{OCH}_3)]_n$ (0.004 mmol) or $[\text{MoO}_2(\text{L})(\text{CH}_3\text{OH})]$ (0.006 mmol) was added along with 30% solution of hydrogen peroxide. The obtained mixture was refluxed for periods of time. Progress of the conversion was continuously monitored by taking samples at regular intervals and running gas or thin layer chromatograms. The products were purified by gas

Table 8. The effect of oxidant on the oxidation of diphenyl sulfide catalyzed by V and Mo complexes in ethanol under reflux.^a

| Oxidant | V complex Conversion (%) after 15 min ^b | Mo complex Conversion (%) after 60 min ^b |
|----------------------------------|---|--|
| No oxidant | 0 | 0 |
| NaIO ₄ | 100 | 95 |
| H ₂ O ₂ | 100 | 100 |
| UHP | 100 | 95 |
| Bu ₄ NIO ₄ | 5 | 10 |
| <i>tert</i> -BuOOH | 5 | 5 |

^aReaction conditions: diphenyl sulfide (1 mmol), oxidant (2 mmol), catalyst (V = 0.004 mmol or Mo = 0.006 mmol), CH₃CH₂OH (10 mL).

^bGC yields.

Table 9. The effect of solvent on the oxidation of diphenyl sulfide with H₂O₂ catalyzed by V and Mo complexes under reflux.^a

| Solvent | V complex Conversion (%) after 15 min ^b | Mo complex Conversion (%) after 60 min ^b |
|--------------------------------------|---|--|
| CH ₃ CH ₂ OH | 100 | 100 |
| CH ₃ OH | 100 | 100 |
| CH ₃ CN | 100 | 100 |
| ClCH ₂ CH ₂ Cl | 100 | 100 |
| CH ₃ COCH ₃ | 55 | 70 |
| CH ₂ Cl ₂ | 0 | 0 |
| CHCl ₃ | 0 | 0 |
| CCl ₄ | 0 | 0 |

^aReaction conditions: diphenyl sulfide (1 mmol), H₂O₂ (2 mmol), catalyst (V = 0.004 mmol or Mo = 0.006 mmol), solvent (10 mL).

^bGC yields.

Table 10. The effect of amount of catalyst on the oxidation of diphenyl sulfide with H₂O₂ catalyzed by V and Mo complexes in ethanol under reflux.^a

| Catalyst amount (mmol) | V complex conversion (%) after 15 min ^b | Mo complex conversion (%) after 60 min ^b |
|------------------------|---|--|
| No catalyst | 0 | 0 |
| 0.003 | 70 | 55 |
| 0.004 | 100 | 90 |
| 0.005 | 100 | 96 |
| 0.006 | 100 | 100 |

^aReaction conditions: diphenyl sulfide (1 mmol), H₂O₂ (2 mmol), CH₃CH₂OH (10 mL).

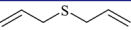
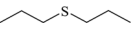
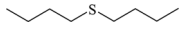
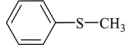
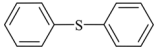
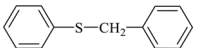
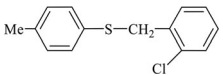
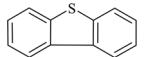
^bGC yields.

chromatography (GC) by packing the column with silica gel as stationary phase and selecting a 70:30 mixture of *n*-hexane and ethyl acetate as mobile phase. The products were identified by comparing their spectral peaks with the library of authentic samples.

Table 8 gives a summary of the effect of oxidants NaIO₄, H₂O₂, urea-hydrogen peroxide (UHP), *tert*-BuOOH and Bu₄NIO₄ on the oxidation of diphenyl sulfide in the presence of [VO(L)(OCH₃)_n] and [MoO₂(L)(CH₃OH)]. The results showed that H₂O₂ is the best source of oxygen and also proved to be inert in the absence of catalyst in ethanol.

The influence of solvent on the rate of catalytic reaction was also studied. For this purpose, ethanol, methanol, acetonitrile, 1,2-dichloroethane, acetone, dichloromethane, chloroform and carbon tetrachloride were tested and the results are given in Table 9. Although the results showed that the reaction performed well in some of these solvents, the ecofriendly nature of ethanol triggered us to use it for our catalytic system.

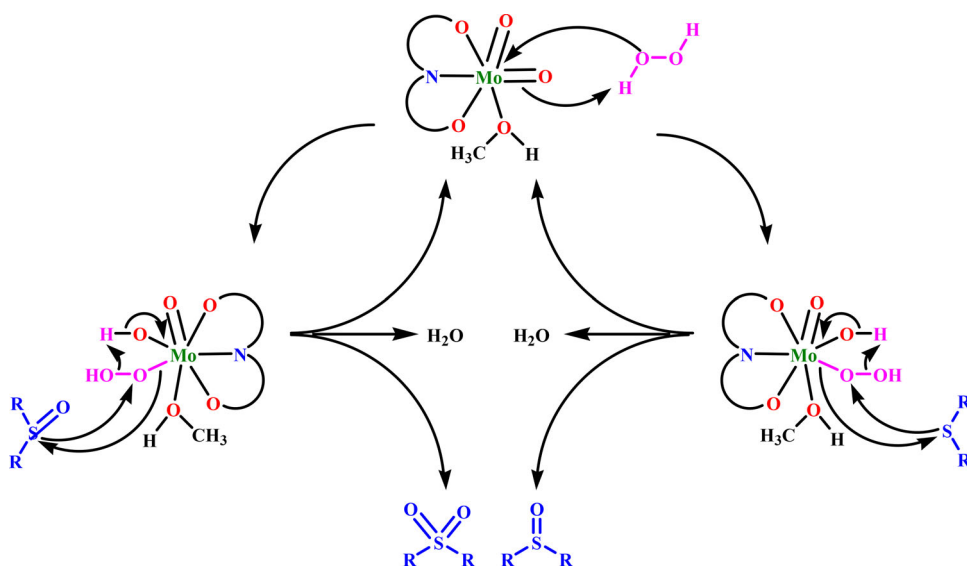
Table 11. Oxidation of sulfides with H₂O₂ catalyzed by V and Mo complexes.^a

| Row | Sulfide | Sulfoxide (%) ^{b,c} | | Sulfone (%) ^{b,c} | | Time (min) | |
|-----|---|------------------------------|----|----------------------------|----|------------|-----|
| | | V | Mo | V | Mo | V | Mo |
| 1 |  | 70 | 80 | 30 | 20 | 15 | 70 |
| 2 |  | 100 | 95 | 0 | 5 | 30 | 30 |
| 3 |  | 100 | 95 | 0 | 5 | 5 | 5 |
| 4 |  | 100 | 70 | 0 | 30 | 10 | 10 |
| 5 |  | 100 | 80 | 0 | 20 | 15 | 60 |
| 6 |  | 90 | 95 | 10 | 5 | 15 | 15 |
| 7 |  | 90 | 70 | 10 | 30 | 30 | 40 |
| 8 |  | 0 | 50 | 0 | 50 | 120 | 240 |

^aReaction conditions: sulfide (1 mmol), H₂O₂ (2 mmol), CH₃CH₂OH (10 mL), catalyst (V = 0.004 mmol or Mo = 0.006 mmol).

^bGC (entries 1–4) or Isolated yield.

^cAll products were identified by comparison of their physical and spectral data with those of authentic samples.



Scheme 3. Plausible mechanism for oxidation of sulfides with H₂O₂ catalyzed by dioxomolybdenum complex.

Examination of the reaction in the presence of different amounts of catalysts showed that the optimal amount of [VO(L)(OCH₃)_n]_n for oxidation of 1 mmol of diphenyl sulfide is 0.004 mmol and for [MoO₂(L)(CH₃OH)] is 0.006 mmol. Diphenyl sulfide was not oxidized in the absence of catalyst as shown by GC (Table 10).

After optimizing the reaction conditions, various aliphatic and aromatic sulfides were oxidized by this catalytic system to get corresponding sulfoxides and sulfones. Table 11 shows that most sulfides were completely converted into their products. In many cases, two different reaction times are reported as time taken by $[\text{VO}(\text{L})(\text{OCH}_3)]_n$ was less than that of $[\text{MoO}_2(\text{L})(\text{CH}_3\text{OH})]$. Also, higher selectivity was observed for vanadium catalyst for the sulfoxide formation over the sulfone. Initially sulfoxides were produced which were gradually converted into sulfones on increasing the reaction time.

Based on previously reported mechanisms, a plausible mechanism for oxidation of sulfides using H_2O_2 catalyzed by $[\text{MoO}_2(\text{L})(\text{CH}_3\text{OH})]$ is proposed as depicted in Scheme 3. Oxidation of sulfides to sulfoxides in the presence of peroxides proceeds through a one-step oxygen-transfer mechanism with simultaneous electrophilic attack of sulfur on one of the oxygens of peroxide, breaking the O–O bond and formation of the S=O bond [52]. Further oxidation, according to the same mechanism, leads to the formation of sulfone. A similar mechanism can also be drawn for the oxovanadium complex.

4. Conclusion

A new tridentate ONO-donor Schiff base ligand and its V(V) and Mo(VI) complexes were synthesized and characterized and the molecular structures were determined by single crystal X-ray crystallography. The coordination geometries around V and Mo were distorted octahedral. Theoretical calculations of H_2L and its V and Mo complexes were performed using DFT at B3LYP/Def2-TZVP level of theory. The theoretical data are in consensus with the experimental data. The catalytic activities of the complexes were performed in oxidation of sulfides with H_2O_2 in ethanol. The present method offers high yield of the products and short time for completion of reaction; higher selectivity was observed for vanadium catalyst for sulfoxide formation over the sulfone.

Acknowledgement

We gratefully acknowledge practical support of this study by Ardakan University and Payame Noor University.

Disclosure statement

No potential conflict of interest was reported by the authors.

ORCID

Hadi Kargar  <http://orcid.org/0000-0002-7817-0937>

Khurram Shahzad Munawar  <http://orcid.org/0000-0001-9055-2519>

Data availability

Crystallographic data for the structural analysis have been deposited with the Cambridge Crystallographic Data Centre as supplementary publication nos. CCDC 2045556 and 2044074 for the vanadium and molybdenum complexes, respectively. Copies of this information may be

obtained free of charge via <http://www.ccdc.cam.ac.uk/conts/retrieving.html> or from the Director, CCDC, 12 Union Road, Cambridge, CB2 1EZ, UK (Fax: +44-1223-336-033; E-mail: deposit@ccdc.ac.uk).

References

- [1] M. Sutradhar, T.R. Barman, E.C. Alegria, M.F. da Silva, C.M. Liu, H.Z. Kou, A.J. Pombeiro. *Dalton Trans.*, **48**, 12839 (2019).
- [2] N. Patel, A.K. Prajapati, R.N. Jadeja, R.N. Patel, S.K. Patel, I.P. Tripathi, N. Dwivedi, V.K. Gupta, R.J. Butcher. *Polyhedron*, **180**, 114434 (2020).
- [3] V. Vrdoljak, M. Mandaric, T. Hrenar, I. Dilovic, J. Pisk, G. Pavlovic, M. Cindric, D. Agustin. *Cryst. Growth Des.*, **19**, 3000 (2019).
- [4] T.M. Asha, M.R. Kurup. *J. Chem. Crystallogr.*, **49**, 219 (2019).
- [5] Y. Li, L. Xu, M. Duan, J. Wu, Y. Wang, K. Dong, M. Han, Z. You. *Inorg. Chem. Commun.*, **105**, 212 (2019).
- [6] S. Mukherjee, S. Chowdhury, A. Ghorai, U. Ghosh, H. Stoeckli-Evans. *Polyhedron*, **51**, 228 (2013).
- [7] K. Figarella, S. Marsiccobetre, I. Galindo-Castro, N. Urdaneta, J.C. Herrera, N. Canudas, E. Galarraga. *Curr. Bioact. Compd.*, **14**, 234 (2018).
- [8] W.Q. Zhang, A.J. Atkin, I.J. Fairlamb, A.C. Whitwood, J.M. Lynam. *Organometallics*, **30**, 4643 (2011).
- [9] I. Sheikhsaie, S.Y. Ebrahimipour, N. Lotfi, J.T. Mague, M. Khaleghi. *Inorg. Chim. Acta*, **442**, 151 (2016).
- [10] A. Hasnaoui, I. Hdoufane, A. Alahyane, A. Nayad, D. Cherqaoui, M.A. Ali, L. El Firdoussi. *Inorg. Chim. Acta*, **501**, 119276 (2020).
- [11] D.C. Crans, J.J. Smee, E. Gaidamauskas, L. Yang. *Chem. Rev.*, **104**, 849 (2004).
- [12] H. Sakurai, Y. Kojima, Y. Yoshikawa, K. Kawabe, H. Yasui. *Coord. Chem. Rev.*, **226**, 187 (2002).
- [13] R.R. Eady. *Coord. Chem. Rev.*, **237**, 23 (2003).
- [14] D. Gambino. *Coord. Chem. Rev.*, **255**, 2193 (2011).
- [15] D. Rehder, G. Santoni, G.M. Licini, C. Schulzke, B. Meier. *Coord. Chem. Rev.*, **237**, 53 (2003).
- [16] K.S. Munawar, S. Ali, M.N. Tahir, N. Khalid, Q. Abbas, I.Z. Qureshi, S. Hussain, M. Ashfaq. *J. Coord. Chem.*, **73**, 2275 (2020).
- [17] K.S. Munawar, S. Ali, M.N. Tahir, N. Khalid, Q. Abbas, I.Z. Qureshi, S. Shahzadi. *Russ. J. Gen. Chem.*, **85**, 2183 (2015).
- [18] H. Hosseini Monfared, S. Kheirabadi, N. Asghari Lalami, P. Mayer. *Polyhedron*, **30**, 1375 (2011).
- [19] M. Sutradhar, A.J.L. Pombeiro. *Coord. Chem. Rev.*, **265**, 89 (2014).
- [20] J. Pisk, J.C. Daran, R. Poli, D. Agustin. *J. Mol. Catal. A Chem.*, **403**, 52 (2015).
- [21] C.J. Schneider, J.E. Penner-Hahn, V.L. Pecoraro. *J. Am. Chem. Soc.*, **130**, 2712 (2008).
- [22] G.H. Spikes, S. Sproules, E. Bill, T. Weyhermuller, K. Wieghardt. *Inorg. Chem.*, **47**, 10935 (2008).
- [23] P.B. Chatterjee, K. Bhattacharya, N. Kundu, K.Y. Choi, R. Clrac, M. Chaudhury. *Inorg. Chem.*, **48**, 804 (2009).
- [24] R.R. Mendel, R. Hänsch. *J. Exp. Bot.*, **53**, 1689 (2002).
- [25] R. Hille, T. Nishino, F. Bittner. *Coord. Chem. Rev.*, **255**, 1179 (2011).
- [26] M. Bagherzadeh, M. Zare. *J. Coord. Chem.*, **66**, 2885 (2013).
- [27] M.E. Judmaier, C. Holzer, M. Volpe, N.C. Mosch-Zanetti. *Inorg. Chem.*, **51**, 9956 (2012).
- [28] L. Gusina, I. Bulhac, D. Dragancea, Y.A. Sinonov, S. Shova. *Rev. Roum. Chim.*, **56**, 133 (2011).
- [29] R. Dinda, P. Sengupta, S. Ghosh, W.S. Sheldrick. *Eur. J. Inorg. Chem.*, 363 (2003).
- [30] E.B. Seenaa, M.R.P. Kurup. *Polyhedron*, **26**, 3595 (2007).

- [31] M. Hatefi, M. Moghadam, I. Sheikhshoei, V. Mirkhani, S. Tangestaninejad, I. Mohammadpoor-Baltork, H. Kargar. *Appl. Catal. A Gen.*, **370**, 66 (2009).
- [32] M. Moghadam, V. Mirkhani, S. Tangestaninejad, I. Mohammadpoor-Baltork, H. Kargar, I. Sheikhshoei, M. Hatefi. *J. Iran. Chem. Soc.*, **8**, 1019 (2011).
- [33] H. Kargar. *Inorg. Chem. Commun.*, **14**, 863 (2011).
- [34] H. Kargar. *Transition Met. Chem.*, **39**, 811 (2014).
- [35] *X-AREA, Version 1.30, Program for the Acquisition and Analysis of Data*, Stoe & Cie GmbH, Darmstadt, Germany (2005).
- [36] *X-RED, Version 1.28b, Program for Data Reduction and Absorption Correction*, Stoe & Cie GmbH, Darmstadt, Germany (2005).
- [37] *X-SHAPE, Version 2.05, Program for Crystal Optimization for Numerical Absorption Correction*, Stoe & Cie GmbH, Darmstadt, Germany (2004).
- [38] R.H. Blessing. *Acta Crystallogr.*, **A51**, 33 (1995).
- [39] M.C. Burla, R. Caliendo, M. Camalli, B. Carrozzini, G.L. Cascarano, L. De Caro, C. Giacovazzo, G. Polidori, R. Spagna. *J. Appl. Crystallogr.*, **38**, 381 (2005).
- [40] G.M. Sheldrick. *Acta Crystallogr.*, **A64**, 112 (2008).
- [41] V. Vrdoljak, B. Prugovecki, D.M. Calogovic, J. Pisk, R. Dreos, P. Siega. *Cryst. Growth Des.*, **11**, 1244 (2011).
- [42] R. Kia, H. Kargar. *J. Coord. Chem.*, **68**, 1441 (2015).
- [43] G. Romanowski, T. Lis. *Inorg. Chim. Acta*, **394**, 627 (2013).
- [44] C. Cordelle, D. Agustin, J.C. Daran, R. Poli. *Inorg. Chim. Acta*, **364**, 144 (2010).
- [45] J. Hartung, S. Drees, M. Grab, P. Schmidt, I. Svoboda, H. Fuess, A. Murso, D. Stalke. *Eur. J. Org. Chem.*, 2388 (2003).
- [46] M. Bagherzadeh, M. Amini, H. Parastar, M. Jalali-Heravi, A. Ellern, L.K. Woo. *Inorg. Chem. Commun.*, **20**, 86 (2012).
- [47] M.R. Maurya, S. Agarwal, C. Bader, M. Ebel, D. Rehder. *Dalton Trans.*, **537** (2005).
- [48] S.D. Kurbah, M. Asthana, I. Syiemlieh, A.A. Lywait, M. Longchar, R.A. Lal. *J. Organomet. Chem.*, **876**, 10 (2018).
- [49] S. Gao, X.-F. Zhang, L.-H. Huo, H. Zhao. *Acta Crystallogr.*, **E60**, m1731 (2004).
- [50] A. Rana, R. Dinda, P. Sengupta, S. Ghosh, L.R. Falvello. *Polyhedron*, **21**, 1023 (2002).
- [51] V. Vrdoljak, M. Cindric, D. Milic, D. Matkovic-Calogovic, P. Novak, B. Kamenar. *Polyhedron*, **24**, 1717 (2005).
- [52] F. Ruff, A. Fabian, O. Farkas, A. Kucsman. *Eur. J. Org. Chem.*, 2102 (2009).